

Novel high pressure magnetic measurements with application to magnetite

Stuart A. Gilder,¹ Maxime LeGoff,¹ Jean Peyronneau,² and Jean-Claude Chervin³

Received 24 October 2001; revised 17 January 2002; accepted 18 January 2002; published 22 May 2002.

[1] We report a novel system designed to measure reversible magnetic susceptibility of micron-sized samples under high pressures in a diamond anvil cell. We find that magnetite reversible hysteresis parameters vary <15% below 0.6 to 1.0 GPa, while at higher pressures significant increases occur in (1) bulk coercivity (Hc) and (2) the ratio of saturation remanent magnetization (Mrs) to saturation magnetization (Ms). The net effect of pressure is to displace magnetite toward a truer single domain state with both higher Mrs/Ms and Hc. Our data, together with the fact that magnetite Curie temperature increases with pressure, suggest that magnetite can account for geomagnetic anomalies related to some subduction zones and potentially to meteorite impact sites on Earth, as well as magnetic signatures observed on some planetary bodies like Mars.

INDEX TERMS: 1540 Geomagnetism and Paleomagnetism: Rock and mineral magnetism; 3994 Mineral Physics: Instruments and techniques; 1519 Geomagnetism and Paleomagnetism: Magnetic mineralogy and petrology; 3924 Mineral Physics: High-pressure behavior

1. Introduction

[2] Magnetite constitutes the most abundant magnetic mineral in the Earth's crust. Its spontaneous magnetization is produced within an inverse spinel structure where superexchange coupling occurs between iron and oxygen ions in two magnetic sublattices (see *Dunlop and Özdemir* [1997] and references therein). The strength of the overall magnetization, characterized by remanent magnetization, susceptibility and coercive force (among others), is governed by inter-atomic distances and angles in each sublattice, and is the sum of magnetocrystalline, magnetostrictive, thermal, strain and magnetostatic (external and demagnetizing fields) energies, all of which are anisotropic and vary with temperature, pressure and external magnetic fields [*Hodoch*, 1976, 1977]. In order to understand the origin of magnetic anomalies measured on or above the Earth's surface, it is important to know how pressure, and thus depth, effects the magnetic properties of magnetite. Most experimental work has employed stresses ≤ 0.8 GPa with the majority being ≤ 0.3 GPa. A comprehensive theory to explain the experimental observations is difficult, however, because the nature of the applied load, be it hydrostatic or uniaxial, and the domain state, composition, size and shape of the studied magnetic minerals, influence the results [*Kear* *et al.*, 1976; *Martin and Noel*, 1988]. For example, magnetization and susceptibility vary less, and are more reversible upon stress release, under hydrostatic loads than under uniaxial loads [*Martin and Noel*, 1988; *Nulman et al.*, 1978; *Kapicka*, 1990].

¹Institut de Physique du Globe, Laboratoire de Paléomagnétisme, Paris, Cedex 05, France.

²Institut de Physique du Globe, Laboratoire de Géomatériaux, Paris, Cedex 05, France.

³Université Pierre et Marie Curie, Physique des Milieux Condensés, Paris, Cedex 05, France.

2. Experimental Design and Theory

[3] To better understand how pressure effects the magnetic properties of materials, we built a system that measures alternating current (ac) susceptibility in a diamond anvil cell that can impose pressures in excess of 30 GPa. The apparatus is similar to that described in *Kim et al.* [1994] with some important exceptions. Our system employed two unequal pick up coils of 351 and 195 turns (Cu wire diameter = 25 μm plus 5 μm of isolation) with diameters of 3 mm and 5.5 mm, respectively that were wound in opposition around a diamond (culet diameter = 370 μm) resulting in a virtually null magnetic surface (Figure 1). Around these was an inducing coil, mounted in null mutual inductance, which produced a peak ac field of 2×10^{-4} T over the sample region. We used a Stanford Research Systems SRS830 lock-in amplifier to measure the output of the sensing coil and a home-made current supply for the inducing coil. Noise at the entrance of the system was <10 nanovolts at acquisition times of 300 milliseconds at an operating frequency of 11.111 kHz. Analytical results were verified to be proportional over frequencies from 1 to 11 kHz with greater sensitivity at higher frequencies. The detection system was housed in a beryllium-copper membranetype diamond cell [*Chervin et al.*, 1995] that was placed in the confines of an electromagnet. Thus the pressure of the cell was remotely controlled and the ac susceptibility was measured as a function of applied field (H), with H varying from -1.2 T to $+1.2$ T.

[4] We studied two natural magnetite samples—one was composed of chiton teeth which are limited to single domain sizes [*Kirschvink and Lowenstam*, 1979] and the other being multidomain grains extracted from a granodiorite [*Gilder and McNulty*, 1999]. Thermomagnetic experiments demonstrated a dramatic decrease in magnetic susceptibility (X) at 580°C in both cases suggesting the samples are Fe-pure (Ti-free). The chiton teeth displayed a marked Hopkinson peak whereas the granodiorite magnetite did not. Samples were loaded together with silica gel into a 200 μm -wide by about 50 μm -deep hole cut in a bronze beryllium gasket. Experimental procedures are shown in Figure 2. The sample+gasket were cycled at least three times through applied fields of ± 1.2 T to obtain X(t,H) (Figures 2a and 2b). To correct for thermal drift (due to room temperature changes, heating from the electromagnet, etc.), we fit a low order polynomial curve to the extremities (≤ -1.15 T and ≥ 1.15 T) and calculated the change in X as a function of time (X'(t)) (Figure 2c), which was then subtracted from the original values (X(t,H) - X'(t)). We then stacked the curves corresponding to the three cycles and calculated the average X - X' at each H (at both increasing and decreasing field directions) (Figure 2d). The same steps were applied to the empty gasket (Figure 2e) at ambient and compressed states before sample loading which was then subtracted from the sample+gasket runs ((X - X')_{sample+gasket} - (X - X')_{gasket})(H) (Figure 2f). Differences among compressed and non-compressed gaskets were negligible and we found no evidence that the coil geometry changed with pressure. The pressure path for the experiments is listed in Table 1. When force was removed from the piston, the shift in the R1 ruby fluorescence spectra [*Adams et al.*, 1976], which was used to calibrate the pressure in the cell, consistently suggested ~ 0.3 GPa residual pressure remained in the sample region after compressing

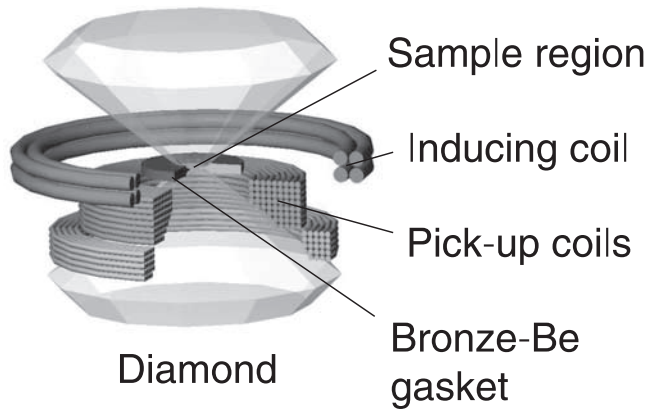


Figure 1. Simplified illustration of ac susceptibility system.

to ~ 0.7 GPa. Hydrostatic conditions in the cell were confirmed by well defined R1–R2 peaks < 3 GPa whereas they tended to broaden thereafter.

[5] When exposed to an external field (H), a ferromagnetic substance acquires a magnetic moment (M) which varies non-linearly until saturation. The value of M depends on whether H is increasing or decreasing: the curve M/H defines a hysteresis loop whose derivative dM/dH is called the differential susceptibility (X_{diff}). When a small ac field is added, M does not follow the full hysteresis loop, but instead defines a minor loop, within the interior of the hysteresis loop, whose slope is less than dM/dH and is called reversible susceptibility (X_{rev}). In other words, X_{diff} changes as a function of H whose integral defines a hysteresis loop ($M(H) = C + \int_{H_0}^H X_{diff}(H) dH$) and has both irreversible and reversible parts ($X_{diff} = X_{irr} + X_{rev}$). Because our technique uses an ac field to measure susceptibility, only the reversible part is recovered. Thus the integral of $X_{rev}(H)dH$ may not fully approach the true (differential) hysteresis loop and may underestimate its associated parameters of saturation magnetization (M_s), remanent saturation magnetization (M_{rs}) and coercivity (H_c). Reversible contributions in magnetite are different in multi- and single domain grains [Dunlop and Özdemir, 1997]. Hysteresis in multidomain magnetite is controlled by the growth of domains whose magnetizations are favorably oriented with the applied field direction, by wall displacement, at the expense of neighboring domains. In contrast, hysteresis of single domain grains is produced by irreversible jumps of the magnetization vector from one easy magnetic axis direction to another closest in line with the applied field direction. Reversibility occurs only before and after a jump, by deviation of the spontaneous magnetization around the easy axis oriented in the H direction. Thus $X_{rev} \rightarrow X_{diff}$ in multidomain magnetite (where H_c and M_{rs} are small), due to the reversibility of wall displacements, while X_{rev} contributes much less to X_{diff} in single domain magnetite. However, despite underestimating X_{diff} values in single domain magnetite, reversible magnetic parameters measured at each pressure increment should be proportional and thus indicative of stress-induced changes in its magnetization.

3. Results, Discussion, and Conclusion

[6] Selected X_{rev} loops for the single and multidomain magnetites are shown in Figure 3 along with the integrals of four loops. In both cases one observes systematic pressure induced changes in amplitude and shape of the X_{rev} curves. Multidomain grains possess one hump at around 0 T whereas the single domain grains have two humps which migrate farther from one another as P increases. The maximum reversible susceptibility ($X_{MAX_{rev}}$) and the integrated $X_{rev}(H)$ parameters are listed in Table 1. $X_{MAX_{rev}}$ generally mimics $M_{s_{rev}}$ as a function of pressure (P) (Figures 4a and 4b). For

multidomain grains, $X_{MAX_{rev}}$ is fairly constant over the first 0.6 GPa; however, it decreased by 80% of its original value from 0.6 to 3.4 GPa. Upon pressure release, $X_{MAX_{rev}}$ lost nearly half of its original value while $M_{s_{rev}}$ lost 25%. Interestingly, upon the second compression series, both $X_{MAX_{rev}}$ and $M_{s_{rev}}$ varied little up to ~ 2.6 GPa, suggesting that the effect of the first compression is to harden the magnetization against stress-induced changes [Carmichael, 1968]. Once a stress is applied that exceeds the previous maximum value, the new $X_{MAX_{rev}}$ and $M_{s_{rev}}$ values follow the trend defined previously at lower pressures. This phenomenon was explained for saturation isothermal remanent magnetization by Boyd *et al.* [1984] who observed that the number of domain walls increased upon initial application of pressure, then the walls rearranged at subsequently higher pressures. After stress was reduced, the domain

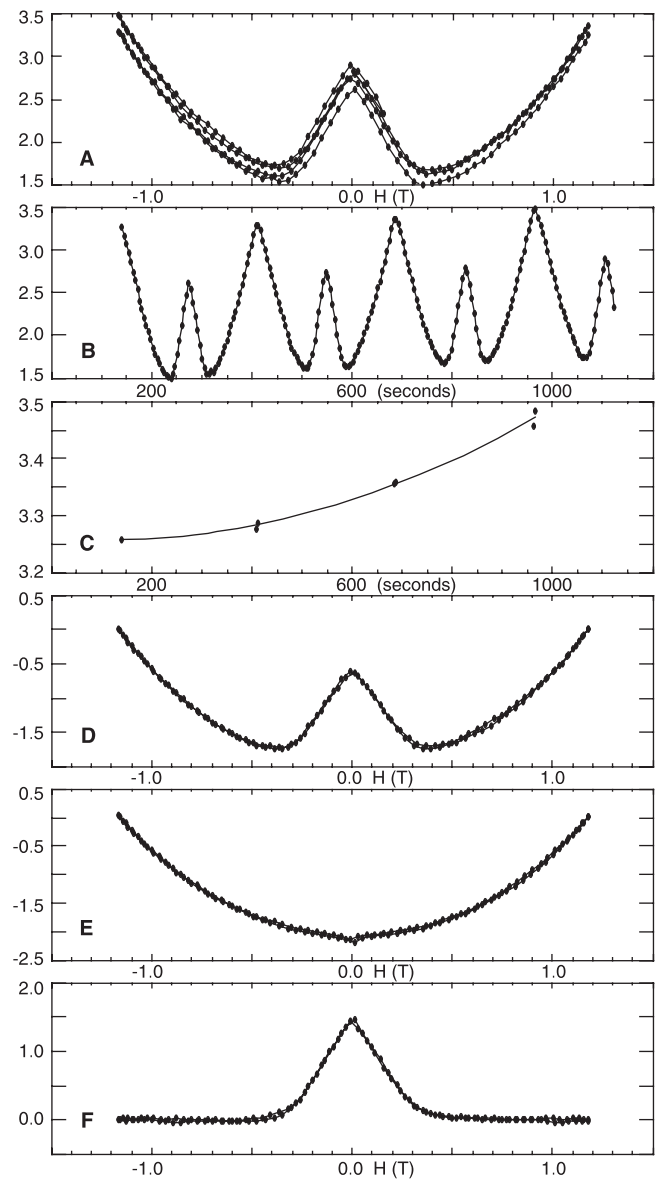


Figure 2. Example of data acquisition and treatment. (a) Susceptibility (arbitrary units) vs. applied field; (b) same susceptibility data in 2a plotted against time, (c) 2nd order polynomial fit to susceptibility data in 2b taken at $H > 1.15$ T and < -1.15 T; (d) susceptibility data in 2a corrected for thermal drift (c) and averaged at each H ; (e) procedure 2a to 2d performed for empty gasket; (f) curve from 2d subtracted by 2e.

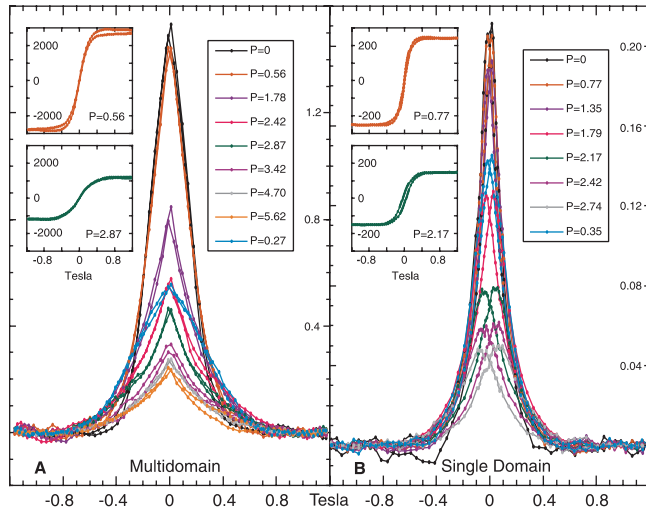
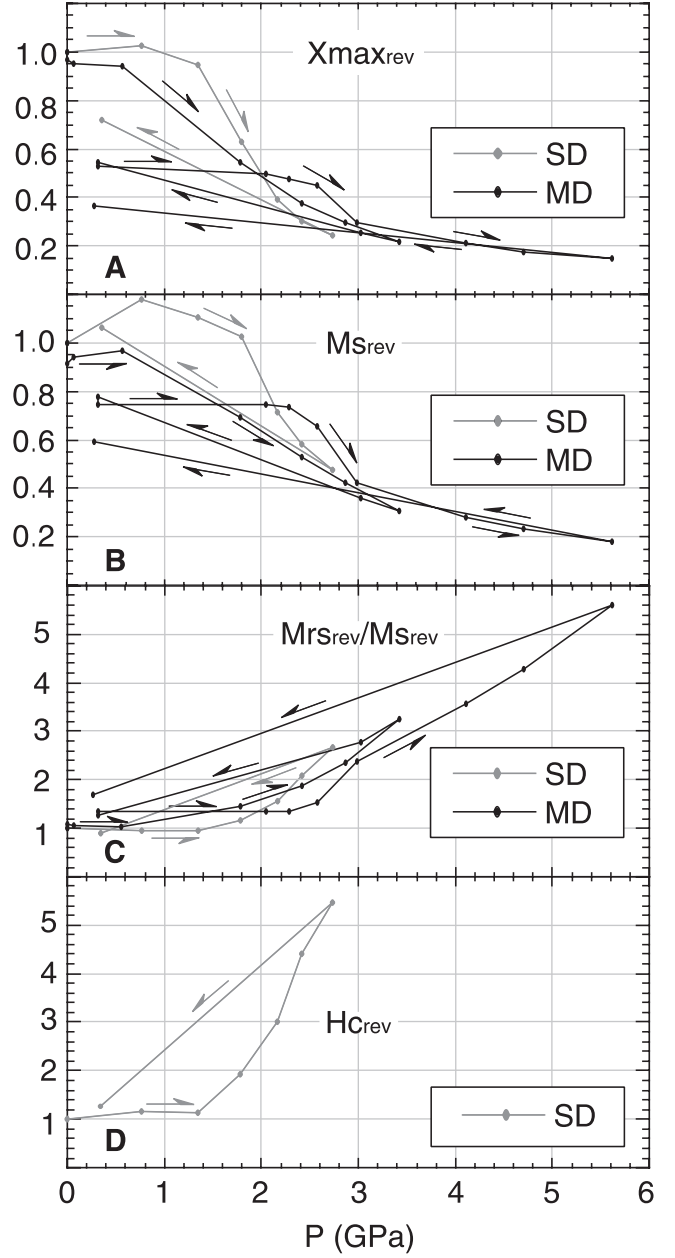
Table 1. Reversible Maximum Susceptibility and Reversible Hysteresis Parameters (Arbitrary Units Unless Specified) from this Study

| Single Domain Magnetite | | | | | |
|-------------------------|-------|-----|------|---------|--|
| P (GPa) | Xmax | Ms | Mrs | Hc (mT) | |
| 0 | 200.5 | 210 | 25.6 | 128.5 | |
| 0.77 | 205.0 | 247 | 28.9 | 148.5 | |
| 1.35 | 190.0 | 232 | 27.2 | 146.5 | |
| 1.79 | 126.0 | 215 | 30.5 | 248.6 | |
| 2.17 | 78.5 | 150 | 28.8 | 387.0 | |
| 2.42 | 60.5 | 122 | 31.0 | 568.0 | |
| 2.74 | 49.0 | 100 | 32.7 | 701.5 | |
| 0.35 | 144.0 | 223 | 24.3 | 162.8 | |

| Multidomain Magnetite | | | | | |
|-----------------------|------|------|------|--------|------|
| P (GPa) | Xmax | Ms | P | Xmax | Ms |
| 0 | 1.49 | 2810 | 0.31 | 0.7867 | 2093 |
| 0.07 | 1.41 | 2645 | 2.05 | 0.7402 | 2088 |
| 0.56 | 1.40 | 2720 | 2.28 | 0.7093 | 2060 |
| 1.78 | 0.81 | 1945 | 2.57 | 0.6684 | 1835 |
| 2.42 | 0.56 | 1490 | 2.98 | 0.4427 | 1183 |
| 2.87 | 0.44 | 1190 | 4.11 | 0.3141 | 790 |
| 3.42 | 0.33 | 865 | 4.70 | 0.2601 | 658 |
| 3.03 | 0.38 | 1013 | 5.62 | 0.2219 | 503 |
| 0.31 | 0.81 | 2185 | 0.27 | 0.5402 | 1665 |

pattern changed irreversibly. Upon a second compression cycle, the domain configuration remained constant and domain motion was reversible within the pressure range of the first compression cycle. By the maximum applied stress (5.62 GPa), X_{MAXrev} and M_{Srev} were <80% of their ambient values. Upon pressure release, X_{MAXrev} and M_{Srev} were ~20% lower than after pressure release from 3.2 GPa and 65% and 40% lower than their original, pre-compressed values. At the resolution of our experiments, we found no significant change in either M_{rsrev} or H_{crev} at any pressure for multidomain grains (values about 10 and 3 mT), which suggests that M_{rsrev}/M_{Srev} rises significantly with increasing pressure (Figure 4c).

[7] For single domain grains, in the first 0.8 GPa X_{MAXrev} changed only slightly while M_{Srev} increased (Figures 4a and 4b). Between 1.0 to 2.8 GPa, both diminished by 70% and 60% of their ambient values, respectively. Upon decompression, X_{MAXrev} and

**Figure 3.** Susceptibility (arbitrary units) vs. applied field in Tesla for (a) multidomain and (b) single domain magnetite as a function of pressure (P) in GPa. In-sets show integrals of corresponding loops.**Figure 4.** Data from Table 1 normalized to pre-compressed ($P = 0$) values; SD = single domain, MD = multidomain, X_{maxrev} , M_{srev} , M_{rsrev} and H_{crev} are the reversible maximum susceptibility, saturation moment, remanent saturation moment and bulk coercivity, respectively. Note that M_{rsrev} was held constant for MD. Also note that two pressure cycles were applied to the same sample of multidomain grains (Table 1).

M_{srev} show greater recovery to pre-compressed values than in the multidomain case. M_{rsrev} slightly increases to 2.8 GPa, and starting at 1.3 GPa, M_{rsrev} / M_{srev} rises with increasing pressure (Figure 4c). Of noted importance is that H_{crev} climbs significantly starting at 1.3 GPa, increasing more than four fold by 2.8 GPa (Figure 4d). Nagata and Kinoshita [1964, 1965] also found that H_c increases with increasing uniaxial stress in titanomagnetite. In their experiments, both M_s and M_{rs} decrease with increasing pressure yet M_{rs}/M_s increases due to the much faster decrease in M_s relative to M_{rs} , as we observed. Their results are similar to ours except that changes in the hysteresis parameters of titanomagnetite occurred at much lower pressures (0 to 0.6 GPa) than for pure

magnetite (>1.0 GPa). This is because magnetostriction coefficients in magnetite increase with increasing titanium concentration which makes titanomagnetite more stress-sensitive than pure magnetite [Nagata, 1966; Nagata and Carleton, 1969; Kean et al., 1976; Pearce and Karson, 1981].

[8] Below 0.6 to 1.0 GPa our experiments show that the magnetic properties of magnetite under hydrostatic stress vary <~15%, whereas significant changes occur above this pressure threshold. These changes can arise from crystalline anisotropy (K_1) and/or magnetostriction (λ_s). In the pressure range considered here, $Fe^{IV} - O$ and $Fe^{VI} - O$ bond distances decrease proportionally while $Fe^{IV} - O - Fe^{VI}$ and $Fe^{VI} - O - Fe^{VI}$ bond angles remain constant [Finger et al., 1986; Haavik et al., 2000], which together suggest that K_1 contributes little to the observed changes in magnetization. On the other hand, because the bulk volume decreases 1%/2 GPa, closer atomic distances should result in heightened superexchange interaction and thus influence λ_s [Hodoch, 1982; Sahu and Moskowitz, 1995]. This is most likely the reason why magnetite demagnetizes faster under uniaxial rather than hydrostatic loads because, for the former, torque on the lattice modifies K_1 in addition to λ_s . Although we do not know the reason for the abrupt change in magnetic parameters above 1 GPa, it can not be due to a phase transition because none has been observed below about 22 GPa. However, slight changes in magnetite's lattice can markedly effect its magnetic properties that theory can not predict. One example is the Verwey transition that occurs when magnetite is cooled below 120°K. At that temperature, the octahedral magnetic sublattice distorts very slightly from cubic to monoclinic symmetry. This distortion orders Fe ions in the sublattice which changes the crystalline anisotropy and results in a higher net magnetization.

[9] For single domain grains, M_{rev}/M_s and $H_{c,rev}$ values increase with increasing pressure, suggesting that the net effect of pressure on magnetite is to make it into a more efficient magnet (e.g., the crystals approach a state of truer single domain behavior characterized by higher M_s/M_r and H_c), which should account for the origin of piezoremanent magnetization. Furthermore, because the Curie temperature of magnetite increases by 20°K/GPa [Samara and Giardini, 1969; Schult, 1970] and because H_c increases with pressure, it is probable that the relaxation time of magnetite also increases with pressure. Thus not only does its magnetization become enhanced due to the piezoremanence effect, but magnetite grains at depth can be more resistant to overprinting, even in the presence of more elevated temperatures. This can potentially explain why magnetic anomalies are associated with some subduction zones [Clark et al., 1985; Arkani-Hamed and Strangway, 1987]. Moreover, some meteorite craters [Hart et al., 1995], which can have magnetic anomalies detectable from satellites, probably owe their origins to shock waves generated at impact. Our results may also play an important role in interpreting the Martian crustal field, which is some eight times stronger than that for the Earth and whose origin may lie at depths exceeding 50 km [Purucker et al., 2000].

[10] **Acknowledgments.** This research was funded by CNRS-INSU and the IGP (BQR). Two anonymous reviewers and several colleagues at IGP provided helpful comments. We thank Joe Kirschvink for providing the chiton teeth and Sonia Rousse for separating the magnetite from the granite. IGP contribution 1806.

References

- Adams, D., R. Appleby, and S. Sharma, Spectroscopy at very high pressures: Part X. Use of ruby R-lines in the estimation of pressure at ambient and at low temperatures, *J. Phys.*, **E9**, 1140–1144, 1976.
- Arkani-Hamed, J., and D. Strangway, An interpretation of magnetic signatures of subduction zones detected by MAGSAT, *Tectonophysics*, **133**, 45–55, 1987.
- Boyd, J., M. Fuller, and S. Halgedahl, Domain wall nucleation as a controlling factor in the behaviour of fine magnetic particles in rocks, *Geophys. Res. Lett.*, **11**, 193–196, 1984.
- Carmichael, R., Remanent and transitory effects of elastic deformation of magnetite 10 crystals, *Phil. Mag.*, **17**, 911–927, 1968.
- Chervin, J., B. Canny, J. Besson, and P. Pruzan, A diamond cell for IR microspectroscopy, *Rev. Sci. Instrum.*, **66**, 2595–2598, 1995.
- Clark, S., H. Frey, and H. Thomas, Satellite magnetic anomalies over subduction zones: The Aleutian arc anomaly, *Geophys. Res. Lett.*, **12**, 41–44, 1985.
- Dunlop, D. and Ö. Özdemir, *Rock Magnetism*, Cambridge Univ. Press, Cambridge, 1997.
- Finger, L., R. Hazen, and A. Hofmeister, High-pressure crystal chemistry of spinel ($MgAl_2O_4$) and magnetite (Fe_3O_4): Comparisons with silicate spinels, *Phys. Chem. Minerals*, **13**, 215–220, 1986.
- Gilder, S., and B. McNulty, Tectonic exhumation and tilting of the Mount Givens pluton, central Sierra Nevada, California, *Geology*, **27**, 919–922, 1999.
- Haavik, C., S. Stölen, H. Fjellvåg, M. Hanfland, and D. Häusermann, Equation of state of magnetite and its high-pressure modification: Thermodynamics of the Fe-O system at high pressure, *Amer. Min.*, **85**, 514–523, 2000.
- Hart, R., R. Hargraves, M. Andreoli, M. Tredoux, and C. Doucouré, Magnetic anomaly near the center of the Vredefort structure: Implications for impact-related magnetic signatures, *Geology*, **23**, 277–280, 1995.
- Hodoch, J., Single-domain theory for the reversible effect of small uniaxial stress upon the initial magnetic susceptibility of rock, *Can. J. Earth Sci.*, **13**, 1186–1200, 1976.
- Hodoch, J., Single-domain theory for the reversible effect of small uniaxial stress upon the remanent magnetization of rock, *Can. J. Earth Sci.*, **14**, 2047–2061, 1977.
- Hodoch, J., Magnetostrictive control of coercive force in multidomain magnetite, *Nature*, **298**, 542–544, 1982.
- Kapicka, A., Variations of the mean susceptibility of rocks under hydrostatic and non-hydrostatic pressure, *Phys. Earth Planet. Int.*, **63**, 78–84, 1990.
- Kean, W., R. Day, M. Fuller, and V. Schmidt, The effect of uniaxial compression on the initial susceptibility of rocks as a function of grain size and composition of their constituent titanomagnetites, *J. Geophys. Res.*, **81**, 861–872, 1976.
- Kim, C., M. Reeves, M. Osofsky, E. Skelton, and D. Liebenberg, A system for in-situ pressure and ac susceptibility measurements using the diamond anvil cell: $Tc(P)$ for $HgBa_2CuO_{4+\delta}$, *Rev. Sci. Instrum.*, **65**, 992–997, 1994.
- Kirschvink, J., and H. Lowenstam, Mineralization and magnetization of chiton teeth: Paleomagnetic, sedimentologic, and biologic implications of organic magnetite, *Earth Planet. Sci. Lett.*, **44**, 193–204, 1979.
- Martin, R., and J. Noel, The influence of stress path on thermoremanent magnetization, *Geophys. Res. Lett.*, **15**, 507–510, 1988.
- Nagata, T., Magnetic susceptibility of compressed rocks, *J. Geomag. Geoelec.*, **18**, 73–80, 1966.
- Nagata, T., and B. Carleton, Notes on piezo-remanent magnetization of igneous rocks III: Theoretical interpretation of experimental results, *J. Geomag. Geoelec.*, **21**, 623–645, 1969.
- Nagata, T., and H. Kinoshita, Effect of release of compression on magnetization of rocks and assemblies of magnetic minerals, *Nature*, **204**, 1183–1184, 1964.
- Nagata, T., and H. Kinoshita, Studies on Piezo-magnetization (I) magnetization of titaniferous magnetite under uniaxial compression, *J. Geomag. Geoelec.*, **17**, 121–135, 1965.
- Nulman, A., et al., Magnetic susceptibility of magnetite under hydrostatic pressure, and implications for tectonomagnetism, *J. Geomag. Geoelec.*, **30**, 585–592, 1978.
- Pearce, G., and J. Karson, On pressure demagnetization, *Geophys. Res. Lett.*, **8**, 725–728, 1981.
- Purucker, M., et al., An altitude-normalized magnetic map of Mars and its interpretation, *Geophys. Res. Lett.*, **27**, 2449–2552, 2000.
- Sahu, S., and B. Moskowitz, Thermal dependence of magnetocrystalline anisotropy and magnetostriction constants of single crystal $Fe_{2.4}Ti_{0.6}O_4$, *Geophys. Res. Lett.*, **22**, 449–452, 1995.
- Samara, G., and A. Giardini, Effect of pressure on the Néel temperature of magnetite, *Phys. Rev.*, **186**, 577–580, 1969.
- Schult, A., Effect of pressure on the Curie temperature of titanomagnetites $[(1-x) \bullet Fe_3O_4 - x \bullet TiFe_2O_4]$, *Earth Planet. Sci. Lett.*, **10**, 81–86, 1970.

S. A. Gilder and M. LeGoff, Institut de Physique du Globe, Laboratoire de Paléomagnétisme, 75252, Paris, Cedex 05, France.

J. Peyronneau, Institut de Physique du Globe, Laboratoire de Géomatériaux, 75252, Paris, Cedex 05, France.

J.-C. Chervin, Université Pierre et Marie Curie, Physique des Milieux Condensés, 75252, Paris, Cedex 05, France.